Int. J. Nonlinear Anal. Appl. 13 (2022) 1, 3113-3129
ISSN: 2008-6822 (electronic)
http://dx.doi.org/10.22075/ijnaa.2021.25343.2989

# Dynamic modeling and microgrid frequency control connecting to the power grid in different modes

Mehrdad Gorjian[a], Mohammad Mehdi Ghanbarian[a,*], Mohammad Hossein Fatehi Dinarlo[a], Mehdi Taghizadeh[a]

[a]*Department of Electrical Engineering, Kazerun Branch, Islamic Azad University, Kazerun, Iran*

*(Communicated by Madjid Eshaghi Gordji)*

**Abstract**

In this paper, using the potential of microgrid surface batteries, the frequency support of the power system in different operating modes was discussed. The study suggested that the process could be supported by a set of batteries in the microgrid (in the mains-connected mode and in the island mode, with the decentralized participation of each, in frequency support (power system or microgrid) in Different operating modes were addressed. The approach used in this paper was to use a convex optimization algorithm. In this way, the batteries independently measured the system frequency and considering their charging mode injected the optimal power into the system, and A convex optimization algorithm will prove that the local optimal point (scattered battery injection) is the optimal point. It will also be universal (optimal system frequency control). Studies in system simulation in two modes of microgrid connected to the main grid and island microgrid have yielded several points.

*Keywords:* Dynamic modeling, microgrid, frequency control, power grid

## 1. Introduction

The 2003 shutdown in North America deprived 55 million people of electricity. In the same year, the blackout plunged the homes of 55 million Italians into darkness. [8] In 2005, the blackouts in 2009 saw the blackout. In 2012, India affected a population of 670 million, with the largest population living in India being the largest population to experience a severe blackout. [6] The

*Corresponding author
*Email addresses:* mehrdadgorjian@ymail.com (Mehrdad Gorjian), ghanbarian@kau.ac.ir (Mohammad Mehdi Ghanbarian), mh_Fatehi@kau.ac.ir (Mohammad Hossein Fatehi Dinarlo), m.taghizadeh@kau.ac.ir (Mehdi Taghizadeh)

*Received:* October 2021 *Accepted:* December 2021

network highlights power more than ever. One of the most essential controls is system frequency control. On the other hand, with the advent of a wide range of scattered products, the power system has improved reliability. However, the control of distributed generation units has added more functional and control complexities to the network, so providing a control approach that provides better performance than existing control approaches can further increase network availability. Ensure safety with the presence of scattered products in the form of microgrids. In this paper, by using the potential available in the batteries available at the network level, the micro frequency network support in different working modes is discussed. [6] The article's proposal is based on the trend that can be achieved with a set of batteries in the microgrid (either low-power batteries on the consumer side or high-power batteries on the supply side of power companies) and with non-participation. Each focuses on supporting the microgrid frequency in different operating modes. [3] The use of energy-saving batteries to support the system frequently causes many problems in terms of battery charge mode and saturation. Various authorities have come up with solutions to these problems [5, 7]. Here, too, the proposed new approach will be able to integrate, in addition to solving saturation and battery charge problems, with optimal and decentralized control of each battery, leading to frequency support with frequency control after turbulence. [10] In this method, we use network-level batteries to solve the problem of saturation in batteries; thus, with the same volume of power as a single battery, we can perform better in addition to the problem of saturation in possible failures and Increasing the reliability of the frequency stabilization system provided. [1] On the other hand, in order to solve the problems caused by battery charge mode, by defining minimizing battery consumption as long as it is within a certain range, as a cost function in an optimal controller to monitor the frequency and make appropriate decisions in the direction. Achieving the objective function in the form of removing the system frequency deviation, an optimal scattered controller is used. Therefore, by controlling the batteries in order to control the frequency of the network, it is possible to ensure the frequency stability of the power system against disturbances. Therefore, providing a control approach that provides better performance than existing control approaches can further ensure the existence of a secure network with the presence of scattered products in the form of microgrids.

## 2. Formulation of The Problem

In this study, fluctuations in production and consumption are not considered. Therefore, the sum of the changes in the transient state is defined by the variable $\Delta e$, according to Equation (2.1). The term $\Delta g_p + \Delta d$ will appear if there is a defect in production or consumption.

$$Imbalance = \Delta e = \Delta g_p \tag{2.1}$$

Given the attribution of total changes to the variable e and the condition that in the event of changes or imbalances between production and consumption, energy storage batteries, by injecting power, will be introduced to eliminate the imbalance between production and consumption. The relationship (2.2) can be shown in order to show the mismatch between production and consumption at any time from time t as follows:

$$u(t) = -\sum_{i \in B} \Delta b_i(t) + \Delta e(t) \tag{2.2}$$

In relation (2.2), $\Delta b_i(t) > 0$ is the injection of power from the batteries into the system and $\Delta b_i(t) < 0$ is the charge of the battery power from the system; $\Delta e(t) < 0$ the imbalance. Positive and $\Delta e(t) < 0$ indicate negative imbalance and thus $\pm u(t)$ indicates excess or lack of power. The number of batteries that will participate in frequency control is shown as $i = \{1, 2, ..., N\}$ The functional

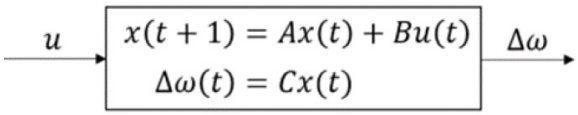


Figure 1: System mode space model

mechanism of the battery controller is that, each battery $i$ measures the frequency deviation $\Delta\omega_i$ and every $t$ seconds in which $t = 0, 1\Delta t, 2\Delta t, 3\Delta t, ...$ relative to the power injection Optimal $\Delta b_i$ to the system will work to remove the frequency deviation. In order to control the frequency, the dynamic model of the studied power system (its state space model) is used according to Figure 1 in a way in which u is modeled as input and $\Delta\omega$ as model output.

Since the presence of random disturbances in any part of the studied power system seems probable, it is necessary to consider a factor in the form of $\xi$ in order to model the disturbance discussed in the power system model. Such disturbances can include:

Disturbance in mechanical performance, modeling, etc. However, the power system model is as follows. It should be noted that there is no measurement noise in relation (2.3).

$$\begin{aligned} x(k+1) &= Ax(k)Bu(k) + \xi(k) \\ \Delta\omega(k) &- Cx(k) \end{aligned} \tag{2.3}$$

As mentioned earlier, it's important to use energy-saving batteries when charging in a range that prevents them from fully filling and discharging. In this paper, in addition to considering such a range for charging mode, it is intended to minimize the use of battery charging as a cost function in an optimal control process. Therefore, the issue of optimization in order to maintain the balance between production and consumption using batteries is defined as follows.

## 3. Optimal frequency control problem

The optimized problem introduced consists of two parts, the first part is the cost function, in this part, minimizing the use of battery charge mode (charging mode consumption) is defined as the cost function. The second part will be subject to the objective, which includes the main discussion of frequency support and the elimination of the imbalance between production and consumption. As discussed in the appendix in detail in relation to optimization issues, the optimization problem leads to the fulfillment of the objective function by minimizing the cost function; in relation to (3.1) the main PP problem in the optimal frequency control discussion is presented. By solving the problem of optimal control of battery consumption, the battery charge or cost function is minimized and the balance between production and consumption, which is the same function of the target, can be achieved.

$$\text{The main problem} = \begin{array}{c} \min_{\Delta b_i} \sum_{i=1}^{N} U_{SOC_i}(\Delta b_i) \\ \text{subject to } \Delta e - \sum_{i=1}^{N} \Delta b_i = 0 \end{array} \tag{3.1}$$

Given the explanations provided, the only possible strategy for solving the problem is to use a central controller. Therefore, the existing solution can be found in the optimization of convexity and in a book of the same name [10]. One source that uses the idea of convex optimization in the power system is [1]. In this reference, the idea of convex optimization has been used in order to unload a set of loads in case of production drop. In this paper, based on convex optimization with

the help of Lagrangian function [11] and the pattern implemented in the reference [1] to control the system frequency (microgrid in island mode and power system in network connection mode, a set of microgrids H), is paid after the disturbance. Appendix A deals briefly with the issue of mathematical optimization and convex optimization.

## 4. Battery charge modes

Given that energy-saving batteries will be used to participate in frequency support, a limit will be applied to the battery charge mode. In this way, in addition to the PP problem becoming a convex problem to solve the scattered approaches as implemented in the previous section, the limitations in the battery charge mode are also met in order to use the batteries effectively.

Condition 1: Battery charge mode $SOC(i,t)$ in the range $[SOC_{\min}(i), SOC_{\max}(i)]$ will be strictly upward.

Note 2: It can be defined according to the definitions provided for a convex set in the appendix, and the ascending state of the battery charge is ascending, based on the $[SOC_{\min}(i), SOC_{\max}(i)]$ convex.

Note 3:

$$SOC_{\min}(i) \leq SOC(i,t) \leq SOC_{\max}(i) \tag{4.1}$$

$$O \leq P_{out}(i,t) \leq \overline{b_i} \tag{4.2}$$

Where $SOC(i,t)$ battery charge mode at time $SOC_{\max}, SOC_{\min}$ battery performance range, $\overline{b_i}$ maximum output at $ith$ battery and finally $P\ out\ (i,t)$ The output power of the batteries will be $Pout_{\max}$ output power according to the maximum allowable limit. Therefore, the condition controller is placed in order to take advantage of the maximum useful life of the battery, so that by increasing the battery charge to a range higher than $SOC_{\max}$, its charging operation stops and in the case of charging $SOC_{\min}$ Also, the battery is exempt from charging for cooperation in order to control the frequency. In this study, the allowable range of battery charge mode is considered to be 0.4 to 0.8. The reason for considering the mentioned range can be explained in such a way that, in case of full and empty battery, the battery life is reduced due to its structural reasons.

## 5. Optimal frequency control problem

The goal of solving the optimization problem was proposed using a convex optimization to provide a decentralized solution to solve the dual problem (cost and purpose function). By taking advantage of the Lagrangian dual function solution, the optimal double problem becomes a problem that will be the so-called double problem. [7] Consider the following standard form for an optimization problem to be solved by the Lagrange dual function:

$$\begin{gathered} \text{minimize} f_0(x) \\ \text{subject to } f_i(x) \leq b_i, i = 1, ..., m \\ h_i(x) = b_i, i = 1, ..., p \end{gathered} \tag{5.1}$$

Lagrange The above equation will be as follows:

$$L(x, \lambda, v) = f_0(x) + \sum_{i=1}^{m} \lambda_i f_i(x) + \sum_{i=1}^{P} v_i h_i(x) \tag{5.2}$$

Where $v_i, \lambda_i$ as the Lagrangian coefficient in relation to $i$ Amin will be the unequal range of $f_i(x) \leq 0$ $ith$ of the equal range in $h_i(x) = 0$. In this case, the variables $\lambda, v$ are called double variables. Reference [4] states that by minimizing the value of the Lagrangian relation (5.2), the Lagrangian double function can be obtained:

$$g_{(\lambda,v)} = \inf_{x \in D} L(x, \lambda, v) = \inf_{x \in D} \left( f_0(x) + \sum_{i=1}^{m} \lambda_i f_i(x) + \sum_{i=1}^{P} v_i h_i(x) \right) \tag{5.3}$$

In order to solve the PP problem, according to what was mentioned in the Lagrange dual function as a method to solve convex optimization problems:

The dual problem referred to in Equation (3.1) is considered and its Lagrangian is calculated using Equation (5.3). It should be noted that in the problem under consideration, there is no unequal condition in the objective function, so there will be no unequal coefficient of $\lambda$.

$$L(\Delta b_i, v) = \sum_{i=1}^{N} U_{-SOC}(\Delta b_i) + v(-\sum_{i=1}^{N} \Delta b_i + \Delta e) \tag{5.4}$$

Then the target function domain will be using the relation (5.3) in the following form:

$$\begin{aligned} g(v) &= \inf_{\Delta b_i \in [\overline{-b_\iota, b_\iota}]} L(\Delta b_i, v) \\ &= \sum_{i=1}^{N} \min_{\Delta b_i \in [\overline{-b_\iota, b_\iota}]} (U\_SOC_i(\Delta b_i) - v\Delta b_i) + v\Delta e \\ &\rightarrow g(v) = \sum_{i=1}^{N} g_i(v) + v\Delta e \end{aligned} \tag{5.5}$$

$$g_i(v) = \min_{\Delta b_i \in [\overline{-b_\iota, b_\iota}]} (U\_SOC_i(\Delta b_i) - v\Delta b_i) \tag{5.6}$$

To achieve the double problem by solving the Lagrangian equations, it is sufficient to obtain the maximum value of $g(v)$; accordingly, we will have:

$DoubleProblem = DP = \max_v g(v)$

$$DP = \max_v g(v) = \sum_{i=1}^{N} g_i(v) + v\Delta e \tag{5.7}$$

According to the reference [2] for each $\underline{v}, \overline{v}$ as follows, the problem presented in (5.7) has at least one optimal point $v \in \left[\underline{p}, \overline{p}\right]$.

$$\begin{aligned} \overline{v} &\geq \max(U_{SOC_i})(\overline{b_i}) \\ \underline{v} &\geq \min(U_{SOC_i})'(O) \end{aligned} \tag{5.8}$$

According to constraints 1 and 2 and meeting the conditions mentioned in [4], instead of solving the PP problem, we can solve the problem of its dichotomy or DP according to the relation (5.7) in order to solve the optimal problem that was initially It was raised, paid. Solve the optimal problem

of Dugan with v, so that by calculating it and placing it as the following relation, we will have the optimal answer for the battery pack.

$$\Delta b_{(v)} = [\Delta b_{1(v)}, ..., \Delta b_{N(v)}]^T \tag{5.9}$$

In connection with the dissolution of relation (5.9), first $v(t)$ must be calculated and by placing it in $\Delta b_i(v(t))$ the value of the optimal power injection of each battery i must be calculated. In the following, the process of solving the optimal control problem will be completed by performing the calculations related to the relation (5.9). It will be, according to what has been said about $v$, that the optimal power change in each battery will be $\Delta b_{i(v)}$, which we will have to calculate:

According to Equation (5.10), which is provided again:

$$g_i(v) = \min_{\Delta b_i \in [-b_i, b_i]} (U\_SOC_i(\Delta b_i) - v\Delta b_i) \tag{5.10}$$

In order for $g_i(v)$ to have a minimum, it must:

$$\begin{aligned} g_i'(v) &= (U\_SOC_i)'(\Delta b_i) - \Delta b_i = O \\ &\rightarrow \Delta b_i(v) = \frac{1}{U\_SOC_i'} \\ \Delta b_i(v) &= \min\left\{\max\left(\frac{1}{U\_SOC_i'(v)}, -\overline{b_i} * step(SOC_{\max} - SOC_i)\right), \overline{b_i} * step(SOC_i - SOC_{\min})\right\} \end{aligned} \tag{5.11}$$

According to clause 1, $U\_SOC_i'$ Will have a derivative in the range $[SOC_{\min}(i), SOC_{\max}(i)]$. In relation (5.11), the allowable range for injecting or recharging the battery (changing the battery power) $(\Delta b_i)$ has been applied. According to [4], using the gradient relationship, $v$ can be calculated and in each time period $t$, the value of $v$ can be updated as follows according to the gradient path $g'(v)$:

$$v(t) = v(t-1) + \gamma g'(v(t-1)) \tag{5.12}$$

Where $\gamma > O$ and the step size determine the changes in $v(t)$. Previously, the result was solved by using the Lagrangian function of relation (5.5), but if we show the changes of each battery $i$ at time $t$ as $\Delta b_i(t) = \Delta b_i(v(t))$, then It follows from Equation (5.5):

$$g(v) = \sum_{i=1}^{N} \min_{\Delta b_i \in [-b_i, b_i]} (U\_SOC_i(\Delta b_i) - v\Delta b_i) + v\Delta e \tag{5.13}$$

In Equation (2.2), the imbalance between production and consumption is defined by ut, and here, too, according to Equation (2.2), the result is:

$$g'(v(t-1)) = -\sum_{i=1}^{N} \Delta b_i(t-1) + \Delta e = u_{t-1} \tag{5.14}$$

## 6. The microgrid is connected to the network

In this case, the nominal power value is considered to be $S_{base} = 200MVA$. For each battery, as mentioned, the injection power (absorption) is limited to (from) the network as follows:

$$i \in B, \Delta b_i \in [-\overline{b_i}, \overline{b_i}] \tag{6.1}$$

## 7. Checking the frequency control of the power system by a set of microgrid surface-level batteries connected to the main grid with the proposed approach

This case study is defined in such a way that a number of microgrids are connected to the main network, the number of $N = 100$ batteries on the network of microgrids has the ability to participate in controlling the frequency of the power grid and considering these conditions and performance. Sustainable system According to the following, the power system is faced with two disturbances in production and reduced production.

$$\Delta g(t) = \begin{cases} 0, & 0 \leq t < 20s \\ 0.05pu, & 20s \leq t \leq 50s \\ 0.15pu, & t \geq 50s \end{cases} \tag{7.1}$$

Now the batteries will be measured locally, and according to the proposed pattern will make the necessary local optimal decision, which according to the proposed approach this optimal local performance will lead to the control of the optimal global frequency.

Figure 2 shows the frequency changes of the power system. The case where the batteries do not play a role in controlling the system frequency is shown in green line. In this case, the dynamics of the system itself, by changing the frequency output, returns it to a permanent state. As can be seen from the figure, the proposed approach will be able to control the frequency of the power system in the best possible control situation in terms of settling time and frequency deviation range. Figure 3 shows the changes in the power drop of the system with the green fold line. To show the battery consumption and how close the proposed approach is to the minimum consumption, the summary diagram of the battery charge usage in Figure 4 is used. The minimum battery charge usage is calculated by the algorithm provided by Stephen Boyd in the MATLAB toolbox. As can be seen, the battery charge usage rate is very close to its minimum value. In subsequent case studies, there will be cases in which the total charge consumption distance is kept to a minimum, in which case it is not possible to expect optimal performance from the proposed approach. Clearly, the batteries will be able to inject power into the system for a limited time, so in Figure 5 the charge mode changes for all 100 batteries during the simulation period. As you can see, the batteries will start from 0.6 to 0.8 from our initial charging mode and will be discharged with the first production drop. The minimum and maximum allowable values for battery charging mode, as mentioned above, are 0.4 to 0.8.

## 8. Check that the system is resistant to modeling changes

In order to test the robustness of the proposed control approach, two complete and approximate modeling are used. For approximate modeling of the system, the batteries are considered by the approximate model of the power system, and in this case the proper performance of the controller can demonstrate the resilience of the control approach. Therefore, the approximate conversion function

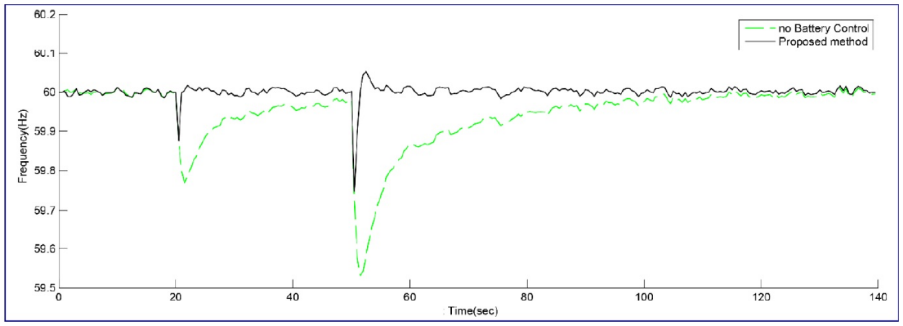


Figure 2: Frequency of battery control system with the proposed approach, black line - uncontrolled, China green line

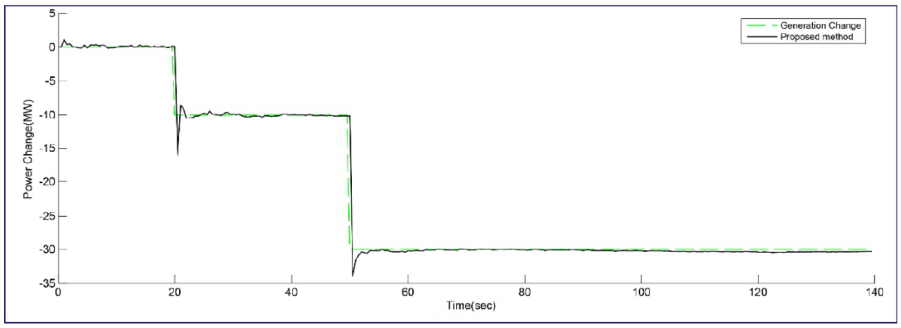


Figure 3: Total power injection into the system by batteries. Proposed approach, black line - change in production, green fold line

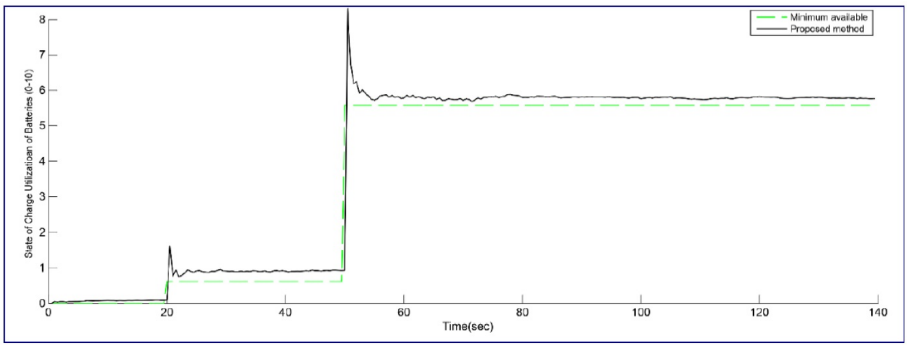


Figure 4: Total use of battery charging mode, suggested approach, black line - at least possible, Chinese green line

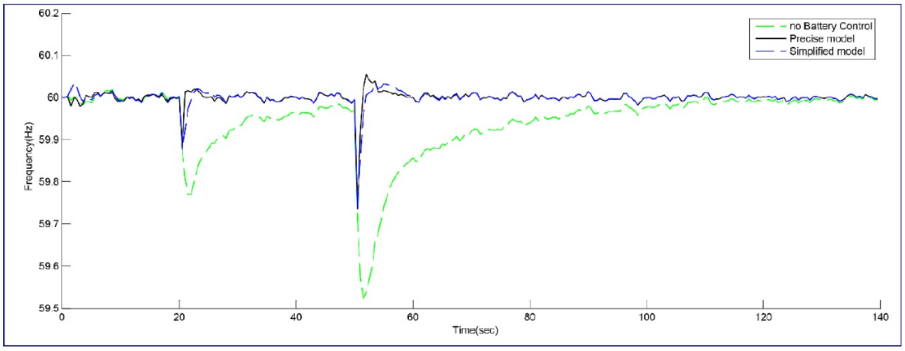


Figure 5: Frequency of battery control system with exact system model, black line - battery control with simplified system, blue fold line - without control, green fold line

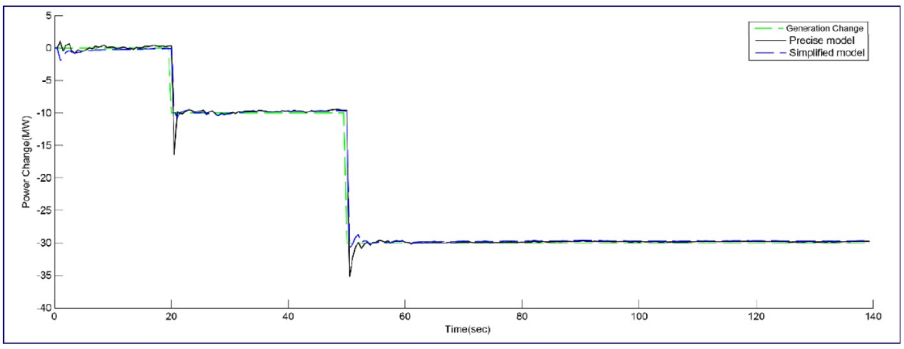


Figure 6: Total injection power into the system by batteries. With precise model, black line - with simplified system model, blue fold line - change in production, green fold line

of the system will be as follows. The simulation results of the exact and inaccurate model of the system are shown in Figures 5 to 7.

$$G(s) = \frac{0.1555s + 0.0222}{S^2 + 0.9918s + 0.4666}$$

Figure 5 shows the frequency changes of the power system. The case in which the batteries use a simplified model to control the system frequency and is indicated by a blue fold line. As can be seen, the performance of the proposed approach in the case of using the simplified model is very close to the use of the complete model. In Figure 6, the batteries are displayed using the model. Finally, in Figure 7, the total use of the battery charging mode is displayed in both the full and approximate model modes. According to the simulation, it can be concluded that the control approach is resistant to modeling changes.

## 9. Check the connection of batteries with each other

In this case, the study aims to investigate the effect of the presence or absence of communication between batteries on controlling the frequency of the power system and minimizing charge consumption. The effect of communication on the frequency control of the power system in Figure 8 is clear. In the event that there is no connection between the batteries, the controller will not be able to achieve optimal global control according to the proposed approach of local optimal control, so optimal performance is not defined for batteries and each battery is not according to its decision or not. The optimal local decision will be charging and discharging, which means that the batteries do

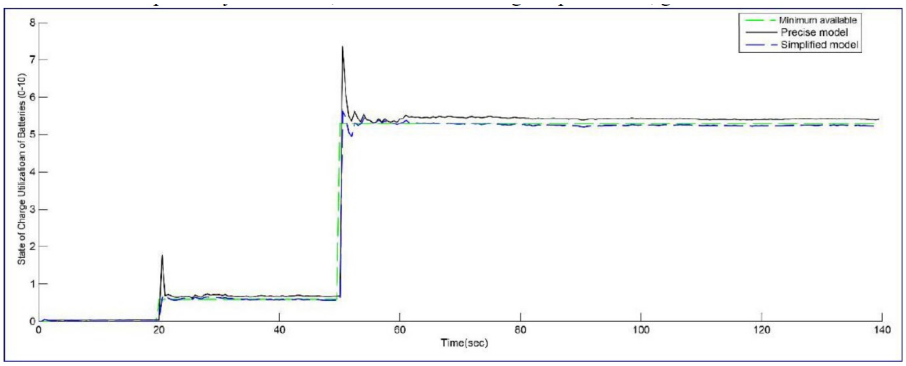


Figure 7: Total use of battery charging mode. Control with precise model, black line - with simplified system model, blue fold line - change in production, green fold line

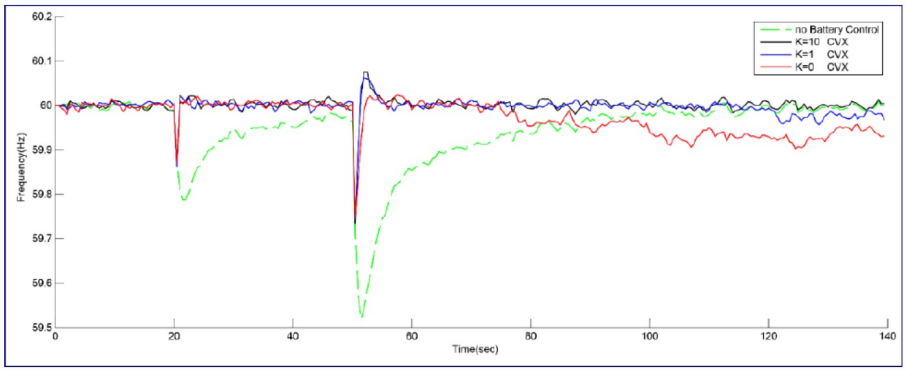


Figure 8: System frequency. The connection of each battery with twenty other batteries ($k = 10$), the black line - the connection of each battery with the other two batteries ($k = 1$), the blue line - the connection of each battery with zero other battery ($k = 0$) - without control, the line Green

not show coherent performance, and much earlier than in cases where there is little communication between them (with the other two batteries), to the state of the state. Charge (0.4 and 0.8). The amount of power injected by the batteries in different cases is also provided in Figure 9. From this figure, it is quite clear that the connection between the batteries leads to the optimal injection of power from the batteries. In the event that there is no connection between the batteries, the high power loss of the batteries is evident. In Figure 10, there is no clear control over the use of battery charge mode in the absence of connection and minimizing charge consumption. The completely inefficient performance of charging consumption is evident in the absence of communication.

## 10. The effect of the number of batteries on the control performance of the proposed approach

The frequency controller function should not be related to the number of batteries involved in frequency control. The only effect of using a small number of batteries will be to increase the use of each battery. In order to confirm the above points, in this case, studies have changed the number of batteries to 200 batteries, 100 batteries, 50 batteries and the results are presented in Figures 11 to 13. Figure 11 shows that in all three cases there was no change in the frequency control of the power system. The amount of power required to compensate for the drop in output in Figure 12 is provided in all three cases of battery counts. The difference between the three modes mentioned in Figure 13 in the amount of battery charge usage will be shown. The higher the number of batteries,

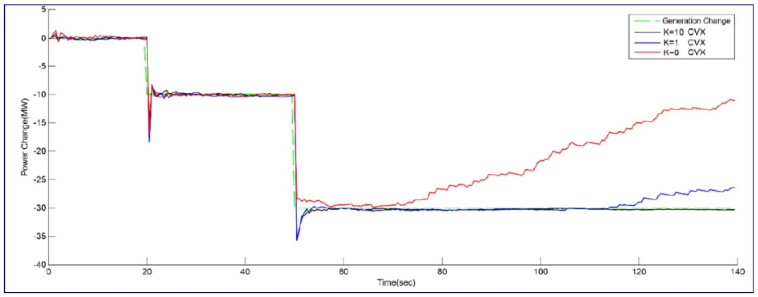


Figure 9: Total injection power into the system. The connection of each battery with the other twenty batteries ($k = 10$), the black line - the connection of each battery with the other two batteries ($k = 1$), the blue line - the connection of each battery with the other zero battery ($k = 0$) - change in production, line Green China

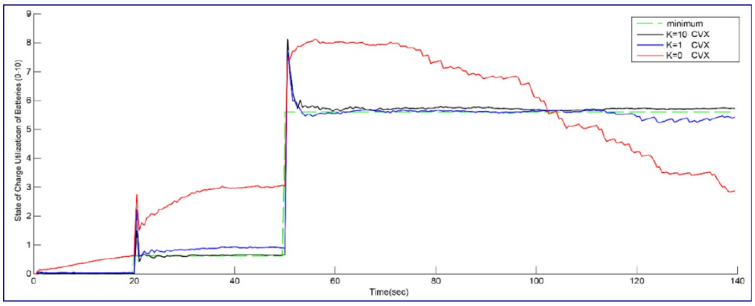


Figure 10: Total use of battery charging mode. The connection of each battery with the other twenty batteries ($k = 10$), the black line - the connection of each battery with the other two batteries ($k = 1$), the blue line - the connection of each battery with the other zero battery ($k = 0$) - change in production, line Green China

the more the charge mode will change with the image ratio. It is clear that in this case, the total power of the batteries is constant.

## 11. Investigating the effect of total battery power on the performance of the proposed approach

As mentioned earlier, according to UCTE, the capacity of auxiliary units to participate in the control of the initial frequency of 1 to 2 MW and the secondary and tertiary control of the frequency of 10 to 20 MW for the 100 MW power system is estimated to be the full volume. The specified power is assigned to the frequency control. Therefore, in this case, studies to study the different states of the total battery power according to the 200 MW power of the power system should be to

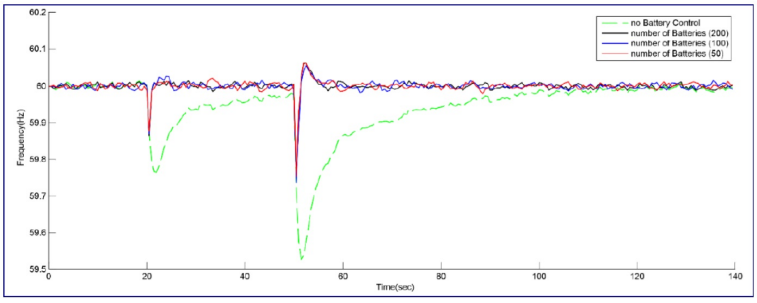


Figure 11: System frequency. Number of batteries 200, black line - number of batteries 100, blue line - number of batteries 50, red line - uncontrolled, green fold line

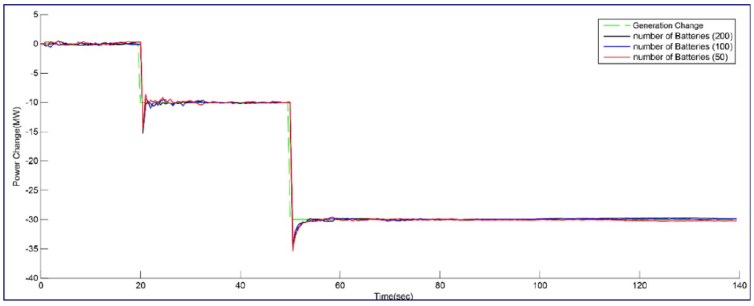


Figure 12: Total power injected into the system by batteries, number of batteries 200, black line - number of batteries 100, blue line - number of batteries 50, red line - change in production, green fold line

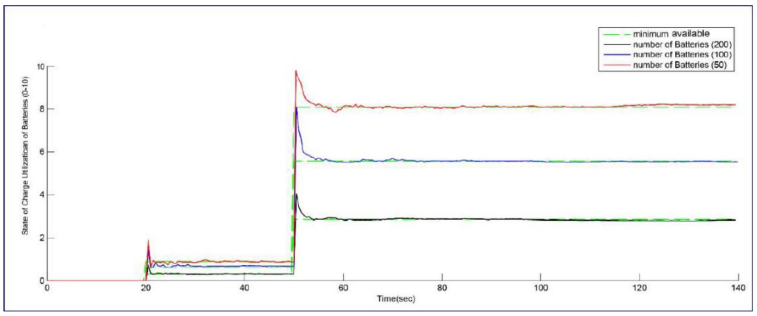


Figure 13: Total use of battery charge mode, number of batteries 200, black line - number of batteries 100, blue line - number of batteries 50, red line - change in production, green fold line

control the secondary frequency of 20 to 40 MW, in this case, studies aimed at testing the power volumes of 40, 30 and 20 MW. For total power, all batteries are considered. Since the worst thing that can happen in a power system is a network outage. Therefore, any mechanism that can save the power system from shutting down can be significant. Table 1, taken from reference [12], introduces the maximum transient frequency deviation of 60 960 MHz. The system's discharge frequency at 60 Hz will also reach 1200 MHz.

Therefore, in this case, studies intend to measure the capability of batteries in the event of major disturbances. Therefore, by changing the turbulence in the system as follows and in total to 45% of the total power of the power system, the performance of the proposed control system is tested. In this case, as described later, the power system shuts down without controlling the batteries.

$$\Delta g(t) = \begin{cases} 0, & 0 \leq t < 20s \\ 0.05pu, & 20s \leq t \leq 50s \\ 0.40pu, & t \geq 50s \end{cases} \tag{11.1}$$

Table 1: Frequency deviations of the power system and related measures

| **Action** | **deviations** | **Frequency** |
|---|---|---|
| Nominal frequency | 0 | 60 Hz |
| Activation of primary control in the power plant | $\pm 24mHz$ | 59.976 Hz-60.024 Hz |
| System malfunction | $\pm 60mHz$ | 59.94 Hz-60.06 Hz |
| The higher the frequency deviation, the longer the state | 240 MHz | 58.56 Hz-60.24 Hz |
| Maximum transient frequency deviation | 960 MHz | 59.04 Hz-60.96 Hz |
| Disinfection | $> 1200MHz$ | 58.8 Hz-61.2 Hz |

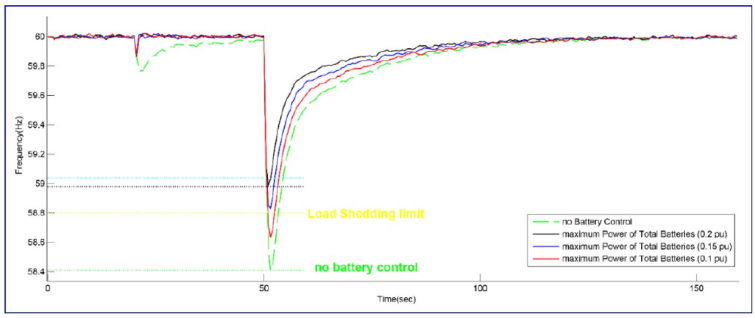


Figure 14: System frequency. Total battery power 0.2 perionite, black line - total battery power 0.15 perionite, blue line - total battery power 0.1 perionite, red line - uncontrolled, green fold line

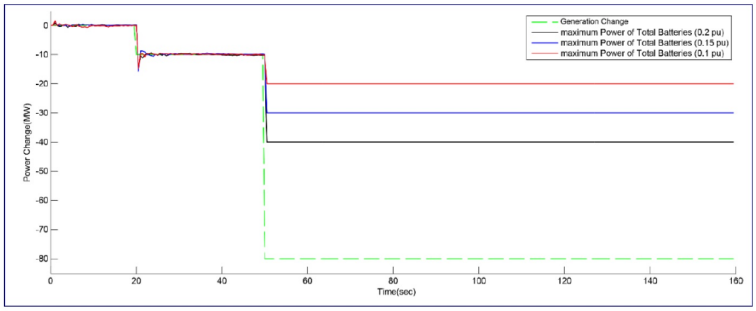


Figure 15: Total injection power into the system. Total battery power 0.2 perionite, black line - total battery power 0.15 perionite, blue line - total battery power 0.1 perionite, red line - uncontrolled, green fold line

It should be noted that the total power of the batteries is determined according to UCTE, 40, 30 and 20 MW and the total production drop is 90 MW ($0.45pu$). Also, we have assumed a loss of production of up to 45% of the total power of the power system due to the display of system performance in different modes. Figures 14 to 16 illustrate the power system with the above assumptions. In Figure 14, as can be seen, the battery control, with a total power of 0.2 pu (black line), maintains the power system in the range farthest from the discharge (frequency 58.8 HZ yellow dotted line). The total power control mode of $0.15pu$ (blue line) has also provided good performance in reducing this power. Control modes with a total power of $0.1pu$ (red line) and uncontrolled (green fold line) have entered the discharge area. Therefore, it was shown that the performance of the system with the necessary power to control the frequency according to UCTE in the drop in unusual power $0.45pu$ will also provide good performance. The highest drop with the UCTE power range ($0.2pu$) for batteries provides performance in the range above the discharge frequency, reaching a total power drop of $0.5pu$. In Figure 15, battery power control, as it turned out, cannot compensate for this power loss (because the output drop is 0.45 pu and the total battery power is $0.1, 0.15, 0.2pu$, but the system is functional Appropriate in two modes of $0.15, 0.2pu$ (black and blue) was able to prevent the frequency from entering the discharge range. The interesting thing about this study is that, with the help of the proposed approach to reducing power up to $0.5pu$, it is also possible to recover with a total battery power of $0.2pu$. Recovery returned to normal without any loss.

## 12. Fall in the Island mode

In the island mode, the microgrid performs very differently than when connected to the network, due to the lack of sufficient inertia in the system. Therefore, the role of frequency control is very important in island mode. The proposed control approach will be able to apply to any type of

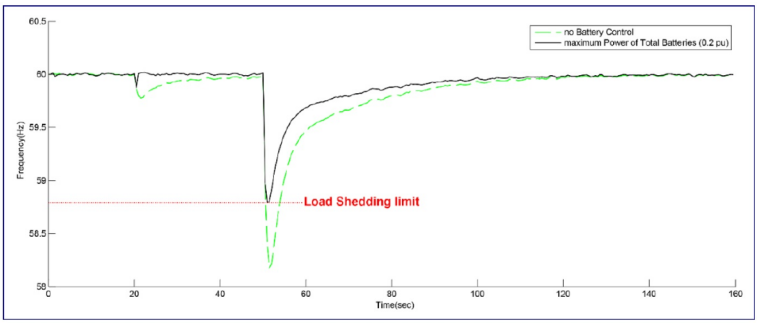


Figure 16: System frequency. Total battery power 0.2 perionite, black line - uncontrolled, green fold line

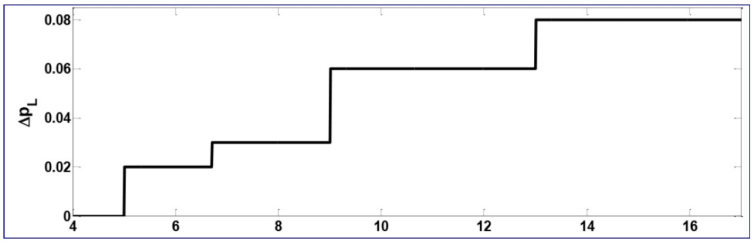


Figure 17: Several consecutive load disturbances

network, including island microgrids, without any changes. In order to investigate the dynamic response of the microgrid system, in spite of the proposed control, the closed-loop system will be examined in the face of several load disturbances, as presented in Figure 17. The system response under the influence of the introduced load disturbances is also provided in Figure 18. $\_P\_L, \Delta f$ are the frequency deviation and the perturbation pattern, the values of which are presented in the pu unit. As shown, the proposed control approach will control the system frequency much better after turbulence than the controllers suggested by the reference [9]. The proposed control approach provides very good performance at the time of subsidence and frequency deviation. As it turns out, the proposed control approach has been able to compensate for the frequency deviation of the first step of the disturbance quickly before the second step occurs, which is not the case in the proposed approach by the reference. To check the performance conditions in the event of a critical state, a $0.1pu$ scale perturbation applied to the system as shown in Figure 20, the proposed approach, in this case, will also provide better performance during subsidence and frequency deviation.

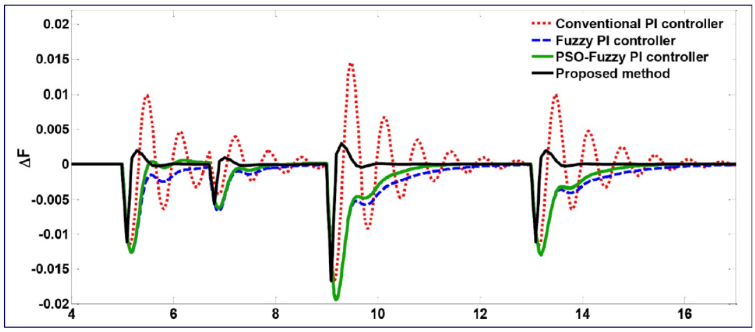


Figure 18: System frequency. In the event of several load disturbances. Proposed approach, black line - PSO-Fuzzy controller, green line - Fuzzy PI controller, blue fold line - PI control red line

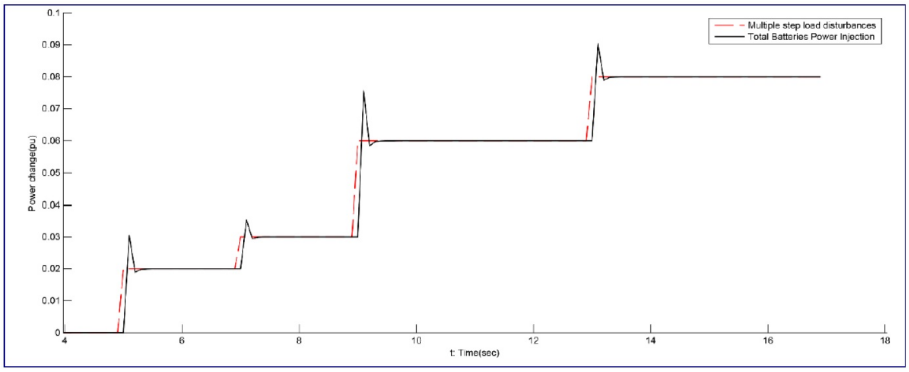


Figure 19: Total power injected into the system by batteries. Proposed approach, black line - several consecutive load disturbances, red fold line

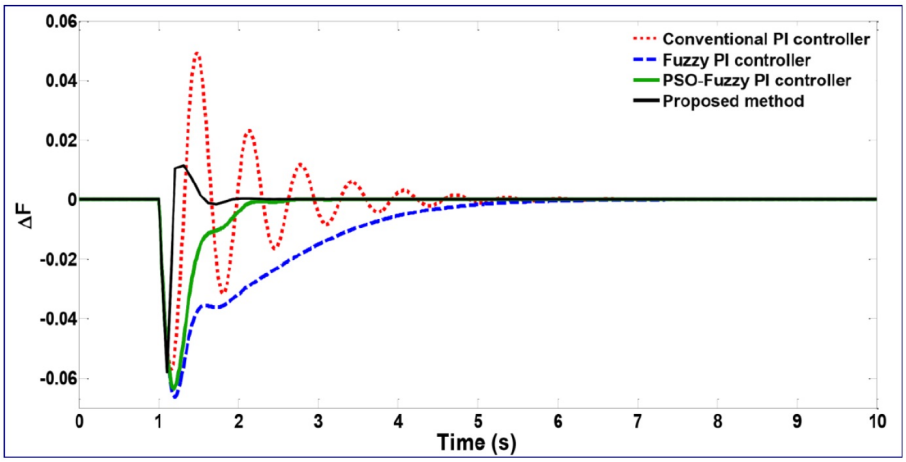


Figure 20: System frequency. In case of disturbance of 0.1 perionite load - Proposed approach, black line - PSO controller - Fuzzy, green line - Fuzzy PI controller, blue fold line - PI control, red fold line

## 13. Conclusion

In this paper, using the potential of microgrid surface batteries, the frequency support of the power system in different operating modes was discussed. The study suggested that the process could be supported by a set of batteries in the microgrid (in the mains-connected mode and in the island mode, with the decentralized participation of each, in frequency support (power system or microgrid) in Different operating modes were addressed. The approach used in this paper was to use a convex optimization algorithm. In this way, the batteries independently measured the system frequency and considering their charging mode injected the optimal power into the system, and A convex optimization algorithm will prove that the local optimal point (scattered battery injection) is the optimal point. It will also be universal (optimal system frequency control). Studies in system simulation in two modes of microgrid connected to the main grid and island microgrid have yielded several points. In the case of connection to the microgrid network, it was shown that the frequency control of the power system by a set of batteries in the microgrid with the proposed approach is able to ensure the stability of the system frequency after the disturbance. It was also shown that the proposed approach was resistant to modeling changes. The effect of battery connection on battery consumption was investigated and it was observed that only by connecting each battery with two adjacent batteries, it is possible to act significantly on the optimal consumption of battery charge. By examining the effect of the number of batteries on the control performance of the proposed approach, the ineffectiveness of the number of batteries on the frequency control of the system as discussed in order to participate in frequency control was examined. In order to show the accuracy of the results on the one hand and to show the performance improvement of the control approach, on the other hand, the simulation results of the control approach were compared with the classical controller and the controller of the predictive model. Was. Examining the micro-network in island performance mode, the stability of the microgrid frequency in the face of turbulence is also in the study. Optimally, in addition to introducing a new idea, it was able to provide better performance than similar existing approaches.

## References

[1] M.R. Aghamohammadi and H. Abdolahinia, *A new approach for optimal sizing of battery energy storage system for primary frequency control of islanded microgrid*, Int. J. Electron. Power Energy Syst. 54 (2014) 333–325.

[2] H. Bevrani, F. Habibi, P. Babahajyani, M. Watanabe and Y. Mitani, *Intelligent frequency control in an ac microgrid: online PSO-based fuzzy tuning approach*, IEEE Trans. Smart Grid 3 (2012) 1944–1935.

[3] A.M. Bouzid, J.M. Guerrero, A. Cheriti, M. Bouhamida, P. Sicard and M. Benghanem, *A survey on control of electric power distributed generation systems for microgrid applications*, Renew. Sustain. Energy Rev. 44 (2015) 166–151.

[4] S. Boyd and L. Vandenberghe, *Convex Optimization*, Cambridge University Press, 2004.

[5] Y. Han, P.M. Young, A. Jain and D. Zimmerle, *Robust control for microgrid frequency deviation reduction with attached storage system*, IEEE Trans. Smart Grid 6 (2015) 565–551.

[6] F. Katiraei, M. Iravani and P.W. Lehn, *Micro-grid autonomous operation during and subsequent to islanding process*, IEEE Trans. Power Delivery 20 (2005) 251–248.

[7] J.-Y. Kim, J.-H. Jeon, S.-K. Kim, C. Cho, J.H. Park, H.-M. Kim and K.-Y. Nam, *Cooperative control strategy of energy storage system and microsources for stabilizing the microgrid during islanded operation*, IEEE Trans. Power Electron. 25 (2010) 3048–3031.

[8] X. Lu, J. M. Guerrero, K. Sun, J.C. Vasquez, R. Teodorescu and L. Huang, *Hierarchical control of parallel AC-DC converter interfaces for hybrid microgrids*, IEEE Trans. Smart Grid 5 (2014) 692–683.

[9] V. Moghadam, R. Mohammad, R.T. Ma and R. Zhang, *Distributed frequency control in smart grids via randomized demand response*, IEEE Trans. Smart Grid 5 (2014) 2809–2198.

[10] J. Pahasa and I. Ngamroo, *PHEVs bidirectional charging/discharging and SoC control for microgrid frequency stabilization using multiple MPC*, IEEE Trans. Smart Grid 6 (2015) 533–526.

[11] I. Serban and C. Marinescu, *Battery energy storage system for frequency support in microgrids and with enhanced control features for uninterruptible supply of local loads*, Int. J. Electr. Power Energy Syst. 54 (2014) 441–432.
[12] A. Teninge, C. Jecu, D. Roye, S. Bacha, J. Duval and R. Belhomme, *Contribution to frequency control through wind turbine inertial energy storage*, IET Renew. Power Gen. 3 (2009) 310–358.